

LA-UR-02-4898

Approved for public release;
distribution is unlimited.

Title: The Milagro All-Sky TeV Gamma Ray Observatory

Author(s): Gus Sinnis

Submitted to: Society of Photo-optical Instrumentation Engineers (SPIE)



Los Alamos National Laboratory, an affirmative action/equal opportunity employer, is operated by the University of California for the U.S. Department of Energy under contract W-7405-ENG-36. By acceptance of this article, the publisher recognizes that the U.S. Government retains a nonexclusive, royalty-free license to publish or reproduce the published form of this contribution, and to allow others to do so, for U.S. Government purposes. Los Alamos National Laboratory requests that the publisher identify this article as work performed under the auspices of the U.S. Department of Energy. Los Alamos National Laboratory strongly supports academic freedom and a researcher's right to publish; as an institution, however, the Laboratory does not endorse the viewpoint of a publication or guarantee its technical correctness.

The Milagro All-Sky TeV Gamma Ray Observatory

Gus Sinnis*

Los Alamos National Laboratory
(For the Milagro Collaboration)

ABSTRACT

Milagro is a water Cherenkov telescope sensitive to gamma rays with energies above 100 GeV. Unlike air-Cherenkov telescopes, Milagro continuously views the entire overhead sky. This capability makes it well suited to search for transient phenomena such as gamma-ray bursts and to discover new phenomena. I will review the design and construction of Milagro, detail the sensitivity of the instrument, including a discussion of background rejection with Milagro. Recent and ongoing upgrades to the instrument are discussed. The paper concludes with a summary of some recent physics results with Milagro.

Keywords: TeV gamma rays, water-Cherenkov detector, all-sky monitor

1. INTRODUCTION

High-energy gamma-ray astronomy is a relatively new field of astronomical exploration. When viewed in TeV gamma rays the universe appears quite different than when viewed optically. The sources of TeV photons are typically non-thermal and contain highly relativistic particles. These sources tend to be episodic or transient in nature. Therefore there is a strong incentive to build an instrument capable of continuously monitoring a large region of the sky in this energy range. Milagro is the first instrument capable of continuously monitoring the entire overhead sky at energies above a few hundred GeV. In this paper I will describe the Milagro detector and discuss the rejection of the cosmic-ray background. The performance and sensitivity of Milagro is demonstrated through observations of the Crab nebula and the active galaxy Mrk 421.

Classic extensive air shower (EAS) arrays consisted of many small scintillation detectors spread over a large physical area. Typically, the sensitive area of the detector covered less than 1% of the physical area of the detector. This sparse sampling of the air shower resulted in rather high energy thresholds: >100 TeV. The CYGNUS¹ and CASA² arrays are examples of such instruments. Despite an apparently anomalous signal from the Hercules X-1³, it is now generally believed that these instruments did not observe any convincing evidence for astrophysical sources of gamma rays at these high energies.

Milagro is a water Cherenkov EAS detector. Unlike scintillation arrays, Milagro densely samples the EAS particles that reach the ground. Since the Cherenkov angle in water is 41° , an array of photomultiplier tubes (PMTs) placed at a depth of roughly $\frac{1}{2}$ their spacing can detect nearly all of the particles that enter the water. In addition, at ground level the gamma rays in the EAS outnumber the electrons and positrons by a factor of ~ 4 . If the PMTs are placed below a radiation length of water these gamma rays can also be detected with high efficiency. These features give Milagro an unprecedented energy threshold for an EAS array. A second layer of PMTs under 16 radiation lengths of water is sensitive to the hadronic component of cosmic-ray induced air showers. At present Milagro rejects roughly 90% of the background cosmic rays while retaining over 50% of the gamma ray events.

Milagro has been operating for 2 years and has detected several astrophysical sources of gamma rays. The Crab nebula is observed as a steady source over the entire period of operation and Mrk 421 has been observed in a flaring state. To date there has been no evidence for TeV gamma-ray emission from gamma ray bursts.

2. THE MILAGRO DETECTOR

The central detector of Milagro is a 6-million gallon water reservoir. The reservoir measures 80m x 60m x 8m deep and is covered with a light-tight cover. Around the central detector an array of 170 water tanks is under construction. The tanks will cover an area of roughly 40,000 m². The detector is located 35 miles west of Los Alamos, NM at an altitude of 2650 m asl (750 g/cm²).

* Contact Gus@lanl.gov; phone (505) 667-9217; fax (505) 665-6943; Los Alamos National Laboratory, MS H803, SM-30 Bikini Atoll Rd, Los Alamos, NM, USA 87545

2.1 The central detector

The reservoir is instrumented with 723 20-cm PMTs (Hamamatsu R5912SEL). The PMTs are deployed in two layers. The top layer of 450 PMTs is under 1.5 meters of water and the bottom layer of 273 PMTs is under 6 meters of water. The PMTs are anchored to a sand-filled PVC pipe by a Kevlar string and set on a 2.8m x 2.8m grid. The sides of the reservoir are sloped (2:1) so that the area of the bottom of the reservoir is smaller than the top, leading to the smaller number of PMTs in the bottom layer. A photograph of the reservoir is shown in Figure 1.

The water in the reservoir should be of good optical clarity, especially near 350 nm (the peak in the sensitivity of the photocathode convolved with the Cherenkov spectrum). A water filtration system cycles water at 200 gallons/minute through a series of filters (10 micron, 1 micron, and 0.2 micron), a UV lamp to kill organisms, and a charcoal filter to remove organic compounds. During the initial filling of the pond the water was processed by a water softener. The attenuation length of the water at 350 nm is 13 meters and has been relatively stable over the past 2 years. Given the depth of the bottom layer (6 meters) there is little to be gained by further improvements in the water quality.

The pond is enclosed in a Faraday cage to protect against lightning strikes to the detector. The cage consists of a mesh of 3/0 and 1/0 stranded hard-copper wire on a rectangular grid spacing of 5.2m x 21 m. The grid covers the pond, the utility building, the counting house, and about 2 acres of surrounding land. While Milagro is situated in one of the most lightning prone regions of the country and several strikes have been spotted close to the detector, to date there has been no lightning induced damage to the instrument.

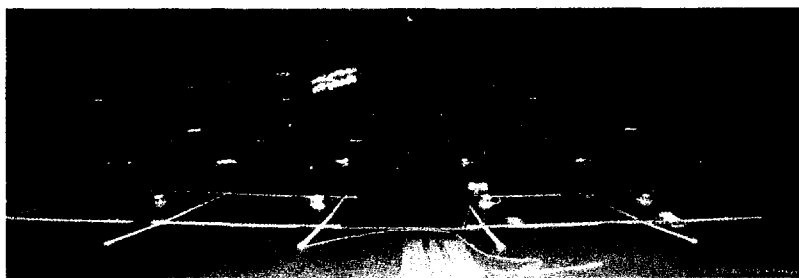


Figure 1. The Milagro detector with the cover inflated for installation.

2.2 Operational experience

A prototype instrument known as Milagruto operated from 1997-1998. The experience gained with Milagruto was crucial in enhancing the performance of the Milagro instrument. Milagruto had a net duty cycle near 80%, there were several major causes for this relatively low duty factor, chief among them was the quality of the power in this rural location. Before commissioning Milagro, a set of uninterruptible power supply (UPS) units was installed to power all of the electronics and data acquisition computers at the experimental site. The other major source of downtime in Milagruto was time taken to calibrate the instrument. In Milagro the data acquisition system was upgraded to allow for simultaneous data taking and calibration runs. The duty cycle of Milagro is now roughly 95%, with 2% of the downtime attributable to scheduled repairs of components in the pond. Figure 2 shows the on-time of the detector averaged over 30-day periods. Before February of 2000, Milagro was running in an "engineering" mode, with a low rate and no real-time reconstruction of the events.

2.3 Event trigger

During most of the previous 2 years of data taking the event trigger was a simple multiplicity trigger, requiring 60 PMTs (in the top layer) to be hit within 180 ns. With this simple trigger, single muons caused the trigger rate to rise steeply below 60 PMTs. The trigger level was set by the capabilities of the data acquisition system, which limited the event rate to roughly 2000 Hz.

Recently an intelligent trigger has been installed that lowers the trigger threshold to 20 PMTs struck in the top layer. Since all of the cables to the top layer of PMTs are the same length (to within a few feet), the signals that arrive at the summing circuitry are in time. Thus, by examining the risetime of the trigger pulse, one can determine how the

trigger was formed. An air shower from near zenith will have all of the PMTs that participate in the trigger struck nearly simultaneously. A single muon will have to traverse a large distance across the pond to generate a trigger. Therefore by requiring the risetime of the trigger to be short, one can remove single muons at the trigger level. Figure 3 shows the risetime of events due to gamma-ray showers and for muon triggers. A clear separation is evident.

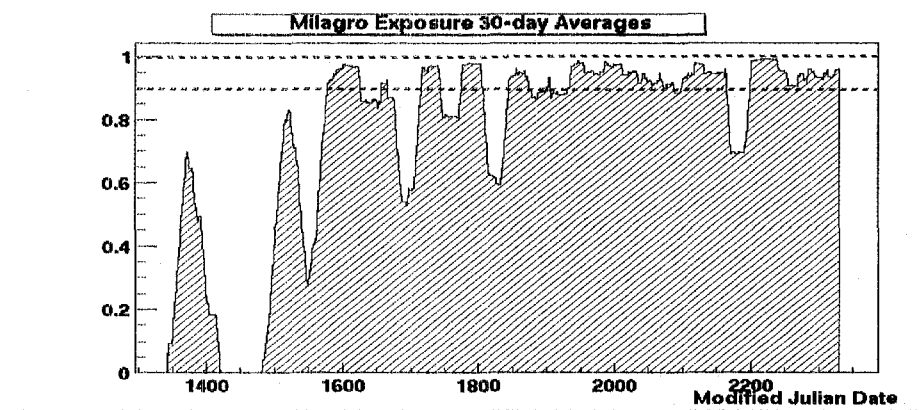


Figure 2. The exposure (or fraction of the time that Milagro was running) as a function of modified Julian date. The data is plotted in 30-day moving averages. The large gap near mjd 1450 was due to a major repair of the underwater connectors. The other glitches are due to an annual scheduled maintenance, the Los Alamos fire, and computer hardware failures.

The trigger is implemented with a flash analog-to-digital converter (FADC) on the trigger signal. The FADC output is stored in a register and the risetime of the trigger is determined by finding the time interval over which 90% of the PMTs in the trigger arrive (5%-95%). At present three triggers are utilized: 1) more than 72 PMTs in the top layer with no restriction on the risetime, 2) more than 50 PMTs in the top layer and a requirement that the risetime be less than 87.5 ns, and 3) more than 20 PMTs in the top layer and a requirement that the risetime of the trigger be less than 50 ns. This trigger has increased the effective area for low-energy (100 GeV) gamma rays by a factor of 4, while keeping the trigger rate below 2000 Hz.

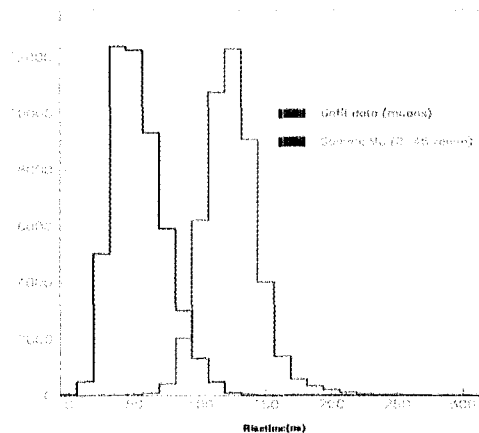


Figure 3. Risetime of gamma-ray triggers, distribution on the left, (from Monte Carlo) and muon triggers, the distribution on the right (from data).

2.3 Real-time data processing

At an event rate of 1700 Hz the data rate from VME is ~5 Mbytes/sec. After compression this is reduced to 2.5 Mbytes/second or about 80 TBytes each year. With present storage technologies (DLT tape) it is impractical to store this entire dataset within the limitations of our budget. Therefore all of the events must be reconstructed in real time. The reconstruction consists of determining the direction, core position, and size of the event, along with any parameters needed to determine the nature of the primary particle (gamma ray or hadronic cosmic ray). This task is performed by an array of Linux-based PCs on a high-bandwidth network. A single PC acquires the data from VME memories. Client processes on the distributed PCs attach to servers on the acquisition computer and obtain blocks of data (typically 100 events). After processing (calibration and reconstruction), the clients return the processed data to the server where they are time ordered and saved to disk. The reconstructed information requires 64 bytes/event. Along with the reconstructed data several other data streams, consisting of the entire raw data from special regions of the sky (the Crab nebula, Mrk 421, the Sun and Moon, events due to single hadron, and any other sources they may be flaring at the time), are stored to disk. This data is transferred to tape for long term storage.

In addition to the special sources and the reconstructed, the entire raw data set is buffered to disk. There is sufficient disk capacity (1.6 TBytes) to buffer 1 week of data. If an interesting event is reported, for example a gamma-ray burst, all raw data taken within 1 hour of the phenomena is saved to tape. This taping system can also respond to alerts generated by Milagro itself (see below).

After the event reconstruction another set of analysis routines search the reconstructed data for gamma ray signals. These routines run on another set of computers and typically access the data within 4 minutes of the event trigger. The analysis routines search for transient signals from any point in the overhead sky over timescales from 250 microseconds to 2 hours. The sky is heavily oversampled as are the timescales searched. If an interesting event is detected an alert is sent to the data archiving system and the raw data within 1 hour of the time of interest is saved. We are currently working on implementing a system to alert the broader scientific community.

2.4 The outrigger array

Water is a very sensitive detection medium for electromagnetic particles. Not only does water provide a medium for the production of Cherenkov light, but also one for the conversion of gamma rays into electrons and/or positrons. On average the PMTs in the reservoir will detect 50% of all electromagnetic particles that enter the pond. This sensitivity allows for the detection of extensive air showers with cores far from the pond (over 100 meters away). The shower front is not a plane, but is cone shaped, with the core of the air shower at the apex of the cone. This effect is known as curvature of the shower front. Therefore, if the core of the air shower is outside of the pond the shower plane will not be perpendicular to the true direction of the primary gamma ray (or cosmic ray). This effect substantially degrades the angular resolution of Milagro. In addition, if the shower core lies outside the pond the energy resolution is extremely poor. A low energy shower with its core close to the pond can lead to the same signal in the pond as a very energetic shower with a distant core.

An array of 177 water tanks (the "outrigger" array) that will surround the Milagro pond is currently under construction. Each tank is a 500 gallon water tank with an area of ~4.6m² and 1m high. The tanks are lined with Tyvek (to reflect the light produced in the tank) and a PMT looks down into the tank. The tanks will be distributed over ~40,000 m² around the pond. The array is scheduled to be complete this Fall/Winter (2002).

By fully containing the EAS, the outrigger array will dramatically improve the angular reconstruction and the energy resolution of Milagro. We expect ~50% energy resolution ($\Delta E/E$) with the complete array of outriggers. As discussed below the background rejection capabilities will also improve with the completion of the outriggers. Overall, the full outrigger array should increase the sensitivity of Milagro by a factor of two.

3. DETECTOR PERFORMANCE

3.1 The shadow of the Moon

The shadow of the Moon in cosmic rays can be used to determine the performance characteristics of Milagro without the use of Monte Carlo simulations. At TeV energies the Moon's shadow is offset from the actual position of the Moon because the cosmic rays are bent in the earth's magnetic field. The bending (amplitude and direction) of a charged particle is a function of the energy, species, and trajectory (zenith angle and azimuthal angle) of the particle. From the position and shape of the observed shadow one can determine the angular resolution of the detector and the absolute energy response of the detector. There is one caveat to the above statements; the angular resolution and energy response are determined for cosmic rays (mostly protons), while one is more interested in the response to gamma rays. However,

the results can be compared to Monte Carlo simulations of the response to hadronic showers and if the observations agree with the simulations, one may have confidence that the simulation of gamma-ray showers and the detector's response to them is also correct.

Figure 4 shows the shadow of the Moon as observed by Milagro. The analysis contains two years of data beginning on February of 2000. The shadow is observed at a significance of $\sim 30\sigma$. Each event has been rotated so that the y-axis is always perpendicular to the direction of magnetic deflection and the x-axis is along the deflection direction. From this figure, the angular resolution to proton induced events is found to be 0.98 degrees, in agreement with Monte Carlo simulations. The angular resolution to gamma ray showers is significantly better than this, 0.8 degrees, simply because gamma ray induced showers that trigger the detector have their cores much closer to the pond than proton induced showers. From the position of the center of the shadow (0.6 degrees from the true position of the Moon) the median energy of triggered proton events is 640 ± 70 GeV (assuming a log normal triggered energy distribution) in agreement with Monte Carlo simulations which predicts a median energy for protons (generated on an $E^{-2.7}$ spectrum) of 690 GeV. (CORSIKA⁴ is used to generate the EAS particles at ground level and GEANT⁵ is used to track these particles and their interactions through the pond, generate the Cherenkov light in the pond, and simulate the response of the detector to the Cherenkov light.) The median energy to gamma rays (generated on an $E^{-2.4}$ spectrum) is somewhat higher, ~ 4 TeV.

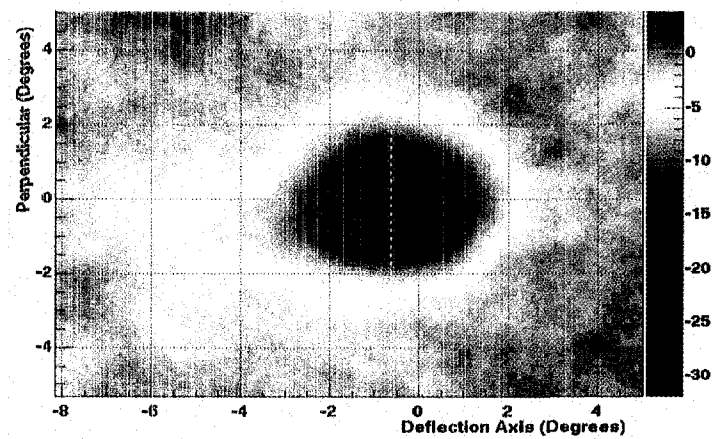


Figure 4. The shadow of the Moon as observed by Milagro. The events have been rotated such that the x-axis is along the direction of magnetic deflection. The asymmetric tail towards the left is due to low energy events. The spread in the y-direction is due to the angular resolution of Milagro.

3.2 Background rejection

The hadronic background from cosmic rays can outnumber the gamma rays by a factor of 1000 to 1 (or more depending upon the angular size of the region examined). The Whipple collaboration has perfected the imaging technique for differentiating between hadronic cosmic rays and gamma ray induced air showers in an atmospheric Cherenkov telescope^{6,7}. In the past year we have developed a technique that uses the information in the bottom layer of Milagro to reject the hadronic background.

Hadronic cosmic rays generate air showers that contain penetrating particles, muons, hadrons that shower in the water, or very energetic electromagnetic particles. Such penetrating particles will deposit a large amount of light in a small region in the bottom of the detector. An air shower that contains no penetrating particles will illuminate the bottom of the detector with a relatively uniform, low level of light. Figure 5 shows three typical proton and gamma ray induced events as viewed in the bottom layer of Milagro. The area of the squares is proportional to the pulse height detected in the PMTs. Small clumps of high light levels are easily distinguished in the proton induced events. We have found a simple parameter, known as *compactness* ($C = N_{\text{PMT}(>2\text{PE})} / \text{PeMax}$ - over the bottom layer), that is sensitive to the differences between proton and gamma ray induced events. The numerator is the number of PMTs in the bottom layer that are struck with more than 2 photoelectrons (PEs) and the denominator is the pulse height, in PEs, of the brightest PMT in the bottom layer. Penetrating particles, that illuminate a small region on the bottom lead to small values of C , while gamma ray events lead to large values of C . Figure 6 shows the C distribution for proton and gamma

ray induced events (from simulations) and data. There is good agreement between data and simulations of proton induced events. Some of the small discrepancy between data and simulations is due to the presence of heavier primary particles in the data (~25% of triggered events are due to He induced air showers), that yield smaller values of C than proton events. The remainder of the difference is most likely due to errors in the simulation of the electronics in Milagro. [Milagro uses a time over threshold method to obtain the pulse height in each PMT. Late light incident on a PMT can mimic a large pulse height in the PMT and therefore an anomalously large value of C . The electronics is (at present) not properly simulated.] By rejecting all events with $C < 2.5$ we reject 90% of the background events while retaining 50% of the gamma ray induced events: an improvement in sensitivity (Q value) of 1.6.

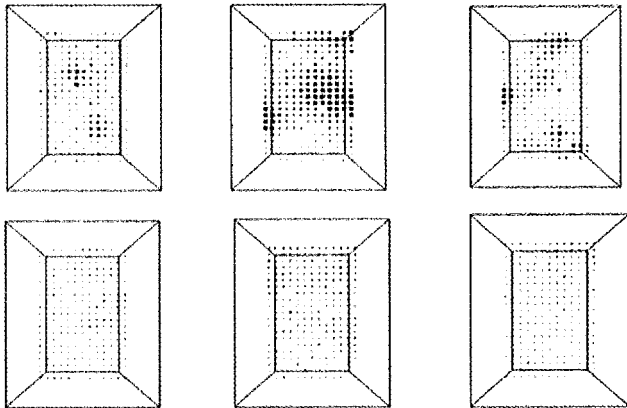


Figure 5. Upper panel shows 3 typical proton events and the lower panel shows 3 typical gamma-ray induced events as observed in the bottom layer of Milagro. The area of the squares is proportional to the measured pulse height in the PMT.

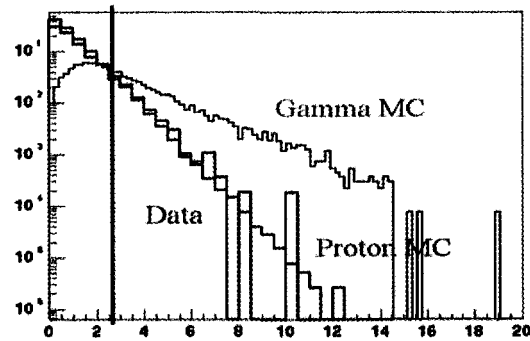


Figure 6. The compactness distribution for data (black curve), Monte Carlo protons (blue), and Monte Carlo gamma rays (red curve). Events to the left of the vertical line are considered background.

The core of a gamma-ray induced air shower can also produce a distinct clump of light in the bottom of the detector. Monte Carlo simulations indicate that the current cut removes a large fraction of gamma-ray showers with cores on the pond. However, for reasons discussed above these events have better angular resolution than events with cores exterior to the pond. Conversely the background rejection for events with cores outside of the pond is better than for events with cores within the pond. With the outrigger array events with cores exterior to the pond will be reconstructed as well as events with cores within the pond. This effect should lead to a substantial improvement in the sensitivity of Milagro (and was included in the estimate for the improvement in sensitivity given above).

4. PHYSICS RESULTS

4.1 The Crab nebula

The Crab nebula was the first source convincingly detected in TeV gamma rays⁸. Since the original detection in 1989 the Crab has become the standard candle of TeV astronomy. The luminosity of the Crab is constant (within the accuracy of the measurements made to date) at⁹ $(2.79 \pm 0.022^{\text{stat}} \pm 0.5^{\text{sys}}) \times 10^{-7} (E/1\text{TeV})^{-2.59} \text{ m}^{-2} \text{ s}^{-1} \text{ TeV}^{-1}$. As a standard candle it is useful for cross calibrating the sensitivity of different instruments.

Milagro has accumulated over 2 years of data on the Crab nebula. Unlike the bulk of the data set, the raw data from the Crab is saved to tape. Therefore as the reconstruction algorithms and background rejection are improved, the data from the Crab can be re-reconstructed over the entire lifetime of the detector. We have analyzed the region around the Crab nebula both with the background rejection discussed above and without the background rejection. The details of the analysis are beyond the scope of this paper. Briefly, since the background cosmic rays are isotropic and the detector response depends solely upon the local coordinates (hour angle and declination), the data can be used to determine the relative sensitivity of the detector as a function of local coordinates. This efficiency is then integrated over the trajectory of the source in the sky, using the instantaneous rate in the detector, to determine the number of expected events from the cosmic-ray background. This is compared with the actual number of events accumulated in the

source bin for evidence of a signal. From the shadow of the Moon and Monte Carlo simulation of the detector the angular resolution of Milagro is 0.8 degrees. The square angular bin that maximizes the significance of a signal has a width 2.8 times the angular resolution of the detector¹⁰. Therefore an angular bin of width 2.1 degrees is used in this analysis. The results of the analysis are given in Table 1.

Using the simulation these results can be used to estimate the flux from the source. Since the energy resolution of Milagro (with the outrigger array) is poor, we do not attempt to fit the spectral index, but instead use the spectral index given by the HEGRA group and estimate the flux. Since the response of the detector is dependent upon the zenith angle of the source, the entire transit of the source must be simulated. Accounting for dead PMTs (on average), the dead time of the detector, the effect of the compactness cut, and the requirement that the event be reconstructed within the angular bin, the simulation yields the following integral for a source transit at the declination of the Crab,

$$I_0 \int A_\gamma(E) \left(\frac{E}{E_{TeV}} \right)^{-2.59} dE = I_0 3.98 \times 10^7 \text{ m}^2 \text{ s TeV day}^{-1} .$$

The excess given in Table 1 corresponds to 9.3 events/day (839 days of exposure) from the Crab. Solving for I_0 yields a flux from the Crab of $2.3(\pm 0.42^{\text{stat}}) \times 10^{-7} (E/1\text{TeV})^{-2.59} \text{ m}^{-2} \text{ s}^{-1} \text{ TeV}^{-1}$ in good agreement with the HEGRA measurement.

	ON Source	Background	Excess	Significance
All Data	16,987,703	16,981,520	6182	1.44
C>2.5	1,952,917	1,945,109	7808	5.4

Table 1. The results of the data analysis from the Crab nebula.

4.2 All-sky survey

As mentioned above the raw data from the entire sky is not saved to permanent storage. Therefore when improved reconstruction algorithms are developed they can not be applied to the data taken from the entire sky. Two major improvements in the reconstruction occurred over the lifetime of Milagro: the development of the background rejection technique and an improvement in the core fitter. The latter is critical to the angular reconstruction of events in an EAS array. Both of these improvements were not available for the online reconstruction until December 15, 2000. Therefore the data discussed here begins on Dec. 15, 2000 and ends on Dec. 15, 2001. In a manner identical to that used to analyze data from the region of the Crab nebula, the entire sky is searched for excesses over the background cosmic rays. The sky is binned into 0.1x0.1 degree bins and the expected background and actual number of events detected in each bin is determined. These small bins are then summed into larger bins, commensurate with the angular resolution of Milagro. Since the beginning of data taking the event rate has been consistently increased. In the beginning of 2000 the event rate was near 1 kHz, by the end of 2001 the event rate was about 1.8 kHz. Along with the event rate increase the angular resolution degraded somewhat. The optimal bin in this analysis was chosen by maximizing the excess from the Crab nebula. This bin is 3.5 degrees wide. The resulting sky map is shown in Figure 7. The circles are drawn around 26 active galaxies identified in Costamante and Ghisellini¹¹ as likely sources of TeV gamma rays, the Crab nebula, Mrk 421, Mrk 501, 1ES1426+428, and 1ES2344+514 (the latter 4 have all been observed at TeV wavelengths by other observatories). The brightest point in the TeV sky over this time period was Mrk 421. Most of the observed signal in this data set came from an outburst that began in December of 2000 and lasted for several months. The next brightest point in the sky is not associated with any of the drawn circles and is to the north-west of the Crab. The location of the maximum excess in this region (ra=79.6, dec=25.8) is near the location of an unidentified EGRET source, 3EG J0520+2556 (ra=80.14, dec=25.75)¹². Given the number of points in the sky viewed by Milagro, the excess at this source, 4.7 σ , is not statistically significant. And while the positional overlap with the EGRET source is interesting, one should be careful before drawing conclusions about the reality of this excess. An examination of the time dependence of this excess shows that the excess was accumulated steadily over the year, consistent with a steady source.

4.3 Gamma-ray bursts in Milagro

Milagrito, a prototype instrument, observed evidence for TeV emission from a gamma-ray burst¹³ detected by BATSE. While this was a relatively strong signal, the poor angular resolution of the BATSE instrument required that a large number of trials be performed to completely search the BATSE error circle. After accounting for all trials the result was significant at the 3 σ level. Since Milagro has been operating the BATSE instrument has stopped acquiring data and the number of GRBs detected by low-energy instruments has dropped markedly. Thus, most of the GRB analysis performed

by Milagro is an “untriggered” analysis. In this type of analysis the entire sky is searched for emission on any timescale between 250 microseconds and 2 hours. No significant events have been detected in the two years of operation of Milagro.

A system has been implemented whereby the data is analyzed within approximately 5 minutes of being acquired. If evidence for a burst is found in the data an automated alert is sent to members of the collaboration. An automated system that can perform quick checks on the data quality and alert the broader scientific community in the case of a significant event is under development.

The sensitivity of Milagro to gamma-ray bursts is dependent on the source emission spectrum and the absorption of high-energy gamma rays enroute to earth via interaction with the intergalactic infrared radiation fields¹⁴. Below 1 TeV the attenuation is strongly energy dependent, at 1 TeV the gamma-ray horizon is below a redshift of 0.1, while at 100 GeV the horizon extends to a redshift of ~ 0.6 . Therefore, it is critical to increase the

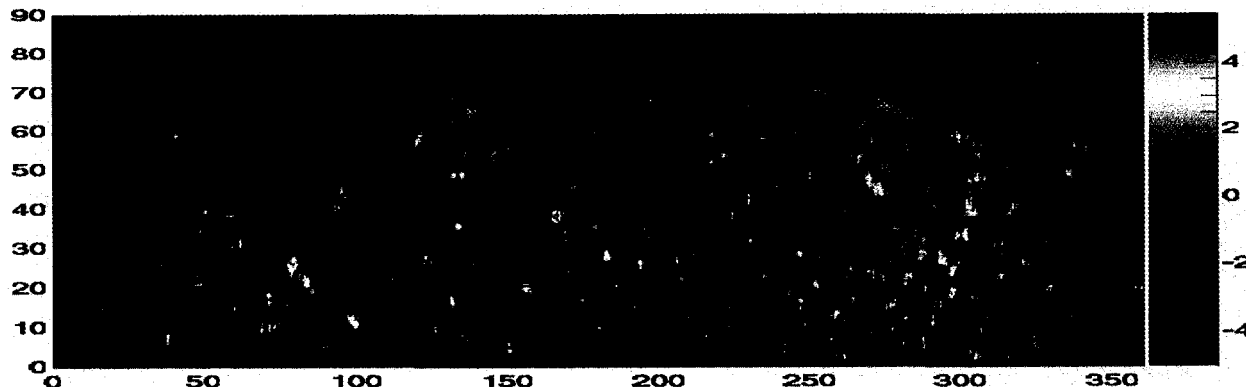


Figure 7. Map of the northern sky in TeV gamma rays. The x-axis is right ascension and the y-axis is declination. The scale is the significance of each point in the sky. The circles mark the locations of AGN and known TeV sources. Mrk 421 is the brightest object in the sky over this data set. The Crab nebula is the third brightest region of the sky. See the text for a discussion of the second brightest region in the northern sky.

sensitivity to low-energy gamma rays. Due to the presence of background the sensitivity of Milagro is a function of the duration of the burst. Figure 8 shows the sensitivity of Milagro as a function of the burst duration under several different assumptions. The lowest curve (best sensitivity) assumes that the source spectrum extends to 2 TeV (with an $E^{-2.4}$ spectrum) and there is no absorption due to the intergalactic radiation fields. The uppermost curve assumes that the observed spectrum at earth has a sharp cutoff at 300 GeV (with an $E^{-2.4}$ spectrum at lower energies) and simulates the simple multiplicity trigger (60 PMTs). This model is appropriate for a source whose emission extends to this energy and lies closer than a redshift of ~ 0.3 . The middle, dashed, curve has the same assumptions about the source spectrum and a cutoff at 300 GeV, but accounts for the new trigger based on the risetime of the event (see section 2.2 for a discussion of this trigger). The points shown in the figure are the measurements of GRB fluence versus duration as measured by BATSE.

6. CONCLUSIONS

The high-energy gamma-ray sky contains only a handful of known sources. Most of the observed sources are transient in nature. To discover new sources, observe flares from the known sources, and possibly see TeV emission from gamma-ray bursts, an all-sky, high duty cycle instrument is needed. Milagro is a new type of extensive air shower array that uses water as the detecting medium. Milagro has been running for over 2 years and has observed 2 sources of TeV gamma rays, the Crab nebula and the active galaxy Mrk 421. Data from the past year has been used to survey the TeV sky, during this period, Mrk 421 was the brightest object in the northern hemisphere. Since commissioning Milagro several improvements have been made to the instrument that has increased the sensitivity to GRBs that lie within a redshift of ~ 0.3 . Data is analyzed in near real-time (~ 5 minute delay) and a system to send alerts to the broader community is in under development. This fall an array of outrigger tanks will be completed which should lead to a two-fold increase in the sensitivity of Milagro.

ACKNOWLEDGEMENTS

This work was supported by the DOE, the National Science Foundation, and Los Alamos National Laboratory.

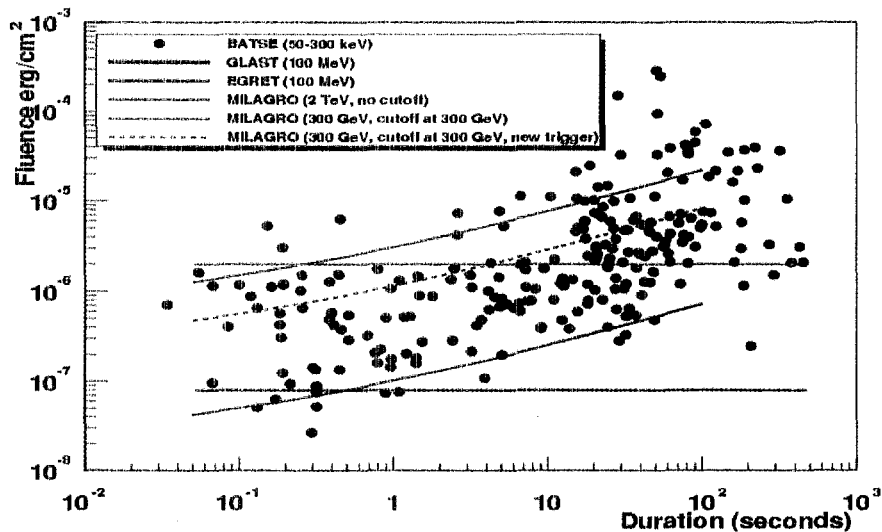


Figure 8. The sensitivity of Milagro to gamma ray bursts. The black circles show the fluence vs. duration for the GRBs detected by BATSE. The lower horizontal line is the expected sensitivity of GLAST to gamma-ray bursts, the upper horizontal line the sensitivity of EGRET. There are 3 curves shown for Milagro. The lowest curve assumes that the intrinsic GRB spectrum extends to 2 TeV and does not account for any absorption of gamma rays. The upper solid curve assumes that no photons survive above 300 GeV. This is roughly equivalent to a GRB lying at a redshift of 0.3. The middle curve (dashed) is the same as the upper curve, but includes the effect of the new triggering system (see section 2.3).

REFERENCES

- Alexandreas, D.E., *et al.*, "The CYGNUS extensive air-shower experiment", *NIM*, A **311**, pp 350-367, 1992.
- Borione, A., *et al.*, "A large air-shower array to search for astrophysical sources emitting g-rays with energies above 10^{14} eV", *NIM*, A **346**, pp 329-352, 1994.
- Dingus, B.L., *et al.*, "Ultra-high-Energy Pulsed Emission from Hercules X-1 with Anomalous Air-Shower Muon Production", *Phys Rev Lett*, **61**, pp 1906-1909, 1988.
- Knapp, J. and Heck, A., "Extensive Air Shower Simulation with CORSIKA: A User's Manual", Kernforschungszentrum Karlsruhe **KfK 5196 B**, 1993. 5. GEANT, CERN Program Library Long Writeup, **W5013**.
- Hillas, A.M., *Proc. of 19th ICRC (La Jolla)*, **3**, pp 445, 1985.
- Weekes, T.C. and Turver, K.E., *Proc. of 12th Eslab Symposium*, eds. R.D. Wills and B. Battrock, pp 279, 1977.
- Weekes, T.C., *et al.*, "Observation of TeV Gamma Rays from the Crab Nebula Using the Atmospheric Cerenkov Imaging Technique", *Ap J*, **342**, pp 379-395, 1989.
- Aharonian, F.A., *et al.*, "The Energy Spectrum of TeV Gamma Rays From the Crab Nebula as Measured by The HEGRA System of Imaging Air Cherenkov Telescopes", *Ap J*, **539**, pp 317-324, 2000.
- Alexandreas, D.E., *et al.*, "Point source search techniques in ultra high energy gamma ray astronomy", *NIM*, **A238**, pp 570-577, 1993.
- Costamante, L. and Ghisellini, G., "TeV Candidate BL Lac Objects", *Astron & Astrophys*, **384** (#1), pp 56-71, 2002.
- Hartman, R.C., *et al.*, "The Third EGRET Catalog of High-Energy Gamma-Ray Sources", *Ap J Supp*, **123**, pp 79-202, 1999.
- Atkins, R., *et al.*, "Evidence for TeV Emission from GRB 970417a", *Ap J Lett*, **533**, pp L119-L122, 2000.
- Stecker, F. W, DeJager, O.D., and Salamon, M.H., "TeV Gamma Rays from 3C 279: A Possible Probe of Origin and Intergalactic Infrared Radiation Fields", *Ap J*, **390**, pp L49-L52, 1992.